2023

Comparison of Cell Cycle Gene Expression Between Ovarian Cancer Cell Line SKOV3 and Non-Cancerous Cell Lines

Akayla Weatherby
Michigan Technological University, aweather@mtu.edu

COMPARISON OF CELL CYCLE GENE EXPRESSION BETWEEN OVARIAN CANCER CELL LINE SKOV3 AND NON-CANCEROUS CELL LINES

By

Akayla J. Weatherby

A THESIS

Submitted in partial fulfillment of the requirements for the degree of

MASTER OF SCIENCE

In Biological Sciences

MICHIGAN TECHNOLOGICAL UNIVERSITY

2023

This thesis has been approved in partial fulfillment of the requirements for the Degree of MASTER OF SCIENCE in Biological Sciences.

Department of Biological Sciences

Thesis Advisor:	*Dr. Paul D. Goetsch*
Committee Member:	*Dr. Robert A. Larson*
Committee Member:	*Dr. Xiaohu (Mark) Tang*
Department Chair:	*Dr. Casey J. Huckins*

Table of Contents

List of Figures

Author Contribution Statement

For this project, Karl Schneider performed the tissue work including the PAR treatment for all cells used, time release from quiescence, and RNA sample collection in TRIZOL. This was done for the cell lines SKOV3, FT282, and BJ5Ta. This work was vital for the completion of this project.

Acknowledgements

I would like to thank Karl Schneider for his assistance in the lab since I could not have done this without his help.

I would also like to thank Dr. Goetsch for all his help and guidance throughout this process over the past year.

Definitions

Cell transformation- the change that occurs when a normal cell becomes malignant

Metastatic- cancer that has spread to multiple areas throughout the body

Pre-cancerous- cells that have grown abnormally resulting in their appearance, size, and shape to be different from normal cells

List of Abbreviations

BJ5Ta- a foreskin fibroblast non-cancerous cell line

BLAST- Basic Local Alignment Search Tool

BUB1- BUB1 Mitotic Checkpoint Serine/Threonine Kinase

CCNB2- Cyclin B2

CDC45- Cell Division Cycle 45

CDK- Cyclin Dependent Kinase

cDNA- Complementary DNA

ddH2O- Double Distilled H2O

DNA- Deoxyribonucleic Acid

dNTP- Deoxyribonucleotide Triphosphate

DREAM- DP, Rb-like, E2F, and MuvB

DYRK1A- Dual Specificity Tyrosine Phosphorylation Regulated Kinase 1A

E2F- transcription factor family

FOXM1- Forkhead Box M1

FT282- a fallopian tube pre-cancerous cell line

LATS1/2- Large Tumor Suppressor Kinases 1/2

MCM5- Minichromosome Maintenance 5

MCM10- Minichromosome Maintenance 10 Replication Initiation Factor

MYBL2- MYB Proto-Oncogene Like 2

NCBI- National Center for Biotechnology Information

ORC1- Origin Recognition Complex Subunit 1

PCR- Polymerase Chain Reaction

PRC1- Protein Regulator of Cytokinesis 1

qPCR- Quantitative PCR

Rb- Retinoblastoma

RNA- Ribonucleic Acid

RNAi- RNA Interference

RT- Reverse Transcription

RT-qPCR- Reverse Transcription Quantitative Real-Time PCR

SKOV3- an ovarian cancer cell line with epithelial morphology

TTK- TTK Protein Kinase

Abstract

Roughly 1% of women will be diagnosed with ovarian cancer during their lifetime. There are many different factors that impact how likely someone is to develop ovarian cancer including age, lifestyle, and family history. Ovarian cancer, like all cancers, occurs due to the accumulation of cancer cells that result from errors in the cell cycle or its regulation. Here, we studied how cell cycle gene expression was altered in the epithelial-like ovarian cancer cell line SKOV3, as compared to the pre-cancerous ovarian cell line FT282, and the non-cancerous foreskin fibroblast cell line BJ5Ta. The three cell lines were synchronized into cell cycle quiescence using CDK4/6 inhibitors for 24 hours before being released into the cell cycle. To compare cell cycle gene regulation between these cell lines, we evaluated the expression of early and late cell cycle genes every two hours following release into the cell cycle using RT-qPCR. The timepoints tested spanned the G1 and S phases of the cell cycle. We observed that the expression of the early and late cell cycle genes tended to be higher in the cancerous cell line at all time points tested, but the regulation of cell cycle genes remained similar between SKOV3 and FT282 cells. However, we observed few changes in cell cycle gene expression over time in BJ5Ta cells, which may indicate that the cell line responds differently to CDK4/6 inhibition that the other cell lines. Our results suggest that although cell cycle gene regulation in SKOV3 cells differs from non-cancerous cell lines, the difference observed was primarily in response to cell cycle quiescence and not in release into the cell cycle. These RT-qPCR results will be used to set up RNA sequencing experiments that will give

further insight into the expression levels of these early and late cell cycle genes, and how cell cycle regulation may differ between cancerous and non-cancerous cells.

1 Introduction

To support an organism's normal development and tissue homeostasis, the cell cycle is tightly regulated. The cell cycle consists of the phases G1, S, G2, and M. Under normal conditions, eukaryotic cells grow continuously during interphase, which consists of the G1, S, and G2 phases. Cells grow during the G1 and G2 phases, and the S phase is when DNA duplication occurs. M phase is mitosis and involves chromosome segregation and cell division [1]. Multiple complexes regulate the transition between phases of the cell cycle. For example, the DREAM complex acts to repress cell cycle gene expression and promotes quiescence while the BMYB-MuvB-FOXM1 complex activates cell cycle genes [16]. Altogether, the balance between repression and activation of the cell cycle ensures regulated cell proliferation within the organism.

Cancerous cells reproduce at a faster rate than what is normally allowed under the regulations of the cell cycle and arise when cell division events no longer properly progress from one stage to the next [5]. In cancer, the balance between DREAM and BMYB-MuvB-FOXM1 is often disturbed to favor BMYB-MuvB-FOXM1 cell cycle activation and cell proliferation [16]. However, most cancer cells retain the capacity to exit the cell cycle, so the DREAM complex maintains function in cancer. Unfortunately, not much is known about the extent to which cancer affects cell cycle gene regulation.

We are interested in understanding how the DREAM complex regulates cell cycle genes in ovarian cancer cells. Ovarian cancer is the eighth most common cancer to occur among women and the 18th most common cancer worldwide [14]. Ovarian cancer is often

diagnosed after it has become metastatic which leads to a lower rate of survival among patients [2]. Many factors, including family history of ovarian or breast cancer, smoking, and ethnicity can all impact the likelihood that someone will develop ovarian cancer [2, 14, 15]. Studies have shown that the incidence of ovarian cancer increases with age with the highest rates seen among women aged 75-79 with a steady increase in cancer rates leading up to this age range [13].

1.1 The Cell Cycle and Cancer

Under normal cell cycle conditions, genetic information is passed from mother to daughter cells in a highly regulated manner. After mitosis, where cells divide in two, G1 phase occurs, and the total genetic function of the cell is checked at restriction points before DNA replication begins. After the cell passes through these restriction points, it has committed to DNA replication during S phase which is followed by the rest phase G2 and quiescence during G0 [12]. When the cell cycle is properly regulated, DNA is accurately duplicated, and the cell divides into identical daughter cells [1]. Many of the processes involved in cell duplication, including DNA replication, monitoring the fidelity of this replication, and the accurate segregation of chromosomes to daughter cells are all characteristically uncontrolled in cancerous cells [29].

DNA is duplicated during the S phase and takes about half of the total time of the cell cycle to be completed in normal mammalian cells. G2 phase happens next and is followed by the shorter M phase, or mitosis, which includes chromosome segregation and cell division. Mitosis begins with chromosome condensation involving packaging

duplicated DNA strands into chromosomes before they are condensed further. The nuclear envelope then breaks down and the sister chromosomes attach to the microtubules of the mitotic spindle. Next, the chromosomes align at the center of the mitotic spindle for segregation of the sister chromatids. The chromosomes then move to opposite poles of the spindle and decondense before the cell is divided in two [1]. Mistakes that occur during the cell cycle or its regulation can result in uncontrolled cell proliferation and cancer [12].

Cyclins and cyclin-dependent kinases (CDKs) are both major regulatory proteins in the cell cycle. CDKs are created throughout the cell cycle and phosphorylate downstream proteins that are essential to normal cell growth. Cyclins are only made at specific points during the cell cycle and act as regulators. If these proteins are not functioning properly, genes that encode tumor suppressor proteins do not function properly either which in turn contributes to cancer development in affected cells [12].

Quiescence is reversible growth arrest where cells can remain in a nondividing state for extended periods of time before reentering the cell cycle. High levels of CDK inhibitors promote quiescence through the inhibition of CDK-cyclin complexes. A transcription factor from the E2F family of transcription factors is sufficient to induce quiescent cells to leave their quiescent state and enter the S phase where DNA is duplicated. Rb can inhibit cell proliferation by binding to and inactivating transcription factor E2F1. However, phosphorylation of Rb by cyclin D-CDK4/6 prevents the ability

of Rb to inactivate E2F [11]. Phosphorylated Rb is not able to inactivate E2F, so cells do not stay quiescent after Rb has been phosphorylated.

1.2 Transcriptional Regulation of the Cell Cycle

The DREAM complex is composed of the dimerization partner (DP), retinoblastoma (Rb)-like, E2F, and MuvB. The MuvB core is composed of proteins LIN9, LIN37, LIN52, LIN54, and RBBP4. The DREAM complex provides a direct link between p130, p107, BMYB, E2F, and FOXM1. The MuvB core binds to p130 and the E2F4-DP1 transcription factor to repress many cell cycle dependent genes when cells are in quiescence [16].

Perturbations in DREAM shifts the balance away from quiescence and towards proliferation which contributes to an increase in gene expression levels that are often associated with poor cancer prognoses. The DREAM complex mediates gene repression during the G0 phase of the cell cycle and coordinates gene expression with expression peaks occurring in both G1/S and G2/M [16]. MuvB binds to p130-E2F-DP to form the DREAM complex during G0 to repress cell cycle dependent gene expression. The protein p130 or p107 forms a multi-subunit protein complex, DREAM, which can repress most to all cell cycle gene expression during quiescence. The MuvB core of the DREAM complex coordinates gene expression during S phase and G2/M through interactions with BMYB and FOXM1. The DREAM complex attaches to binding sites near the transcription start site of many cell cycle genes. Disruption of DREAM complex

components through RNAi or mutations can lead a loss in the gene repression necessary to maintain quiescence [16].

The MuvB core contains LIN9, LIN52, LIN37, LIN54, and RBBP4. The DREAM complex binds to and represses cell cycle genes that maximally express during S, G2, and M phases due to the interaction between DREAM and cell cycle gene homology region (CHR) promoter elements. Following this, MuvB interacts with BMYB and FOXM1 and switches from being a transcriptional repressor to an activator. The BMYB-MuvB (MMB) complex forms during S phase and is necessary for beginning transcriptional activation and recruiting FOXM1. The FOXM1-MuvB complex stimulates the expression of cell cycle genes during G2/M phases. The DREAM complex is necessary for the repression of cell cycle genes through the binding of CHR and E2F sites during quiescence and the loss of DREAM activity is not compensated for by other repressor complexes [9].

For the DREAM complex to assemble, an intact serine 28 residue on LIN52 is necessary for p130 to bind MuvB. The importance of this residue is supported by the fact that a mutant serine 28 in LIN52 caused cells with this mutant residue to have a reduced ability to enter quiescence when compared to cells with an intact serine 28. DYRK1A can phosphorylate S28-LIN52 and recruit p130 to MuvB to form the DREAM complex. It is suggested that p130 has a repressive role in E2F dependent transcription because of high expression levels of p130 during quiescence and low levels in proliferating cells. The repressive role of p130 is supported by its binding to the repressive transcription factors

E2F4 and E2F5. The binding of p130 to the MuvB core can be disrupted by the binding of viral oncogenes to p130 [16].

The Rb protein is needed to properly regulate the cell cycle. Mammalian cells without functional Rb are still able to quiesce if DREAM is functional due to the overlapping function between Rb family proteins and the DREAM components p107 and p130. Gene expression needed for cell cycle progression during G0 and early G1 is repressed by interactions between E2F and Rb family proteins. It is suggested that the MuvB component LIN37 cooperates with Rb to initiate quiescence and cells negative for both LIN37 and Rb are essentially unable to exit the cell cycle. Knockout of Rb and LIN37 deregulates the expression of cell cycle genes and leads to a loss of control of the cell cycle and the inability of cells to enter quiescence as a response to growth-inhibiting conditions. Following these conditions, expression of Rb and the MuvB component LIN37 together can rescue promoter repression [9].

The balance between the proliferative phase BMYB-MuvB-FOXM1 complex and quiescent DREAM complex is often disturbed in cancerous cells. In some cancerous cells, DREAM is lost and the activity of BMYB-MuvB-FOXM1 increases and pushes cells to proliferate. The loss of FOXM1 delays entry into mitosis and causes abnormal mitosis and cytokinesis. In addition to this, the loss of FOXM1, MuvB, and BMYB all result in similar phenotypes. Increased levels of BMYB and FOXM1 are associated with poor outcomes in some cancers. Overexpression of these cell cycle genes could alter the balance between the DREAM and BMYB-MuvB complexes in cells. BMYB and

FOXM1 could be at high levels in cells that have compromised DREAM function due to the loss of LATS1/2, DYRK1A, p130, or p107. Loss of DYRK1A would reduce p130 recruitment to MuvB to form the DREAM complex, and loss of the kinases large tumor suppressors LATS1/2 compromises p130 binding to MuvB and reduces the ability of cells to become quiescent. The tumor suppressor protein p53 shifts cellular levels in favor of p130-DREAM over BMYB. This shift from BMYB-MuvB towards DREAM is due to the p53-dependent induction of p21 which inhibits cyclin A-CDK2 dependent activation of both BMYB and FOXM1 while also reducing the phosphorylation levels of p130. The switch from DREAM to MuvB is normally highly regulated with the MuvB core recruiting BMYB during S phase and recruiting FOXM1 during G2. DYRK1A plays an essential role in the binding of p130 to the MuvB core, enabling the formation of the DREAM complex and permitting cells to exit the cell cycle and enter quiescence. DREAM can be disrupted by deregulated cyclin and CDK activity or Rb resulting in the expression of cell cycle genes that are dependent on E2Fs and the activation of late cell cycle genes. Activator E2Fs are needed for G1/S genes to be expressed, and the MuvB core, FOXM1, and BMYB are all needed for G2/M genes to be expressed [16]. Cancerous cells can arise when the expression of cell cycle genes is no longer properly regulated.

1.3 Ovarian Cancer

Based on data from 2017-2019, about 1.1% of women will be diagnosed with ovarian cancer during their lifetime. From 2016-2020, 10.3 new ovarian cancer cases per 100,000 women per year and a death rate of 6.3 women per 100,000 per year was

recorded. There were an estimated 236,511 women living with ovarian cancer in the United States alone in 2020 [4]. Roughly 22,000 women in the US are diagnosed with ovarian cancer every year [15].

The incidence of ovarian cancer varies by race with the highest incidence being among women who are non-Hispanic and White and the lowest incidence among Asian/Pacific Islanders and non-Hispanic Black women [15]. It has been shown that from 15-19 the incidence rates of ovarian cancer increase steadily until 40-44 where the increase in incidence becomes more extreme until 75-79. After 75-79, the incidence rates begin decreasing quickly [13]. Other factors, including being tall, overweight, and not bearing children have all been associated with an increased risk for developing ovarian cancer, but the strongest risk factor is a family history of either breast or ovarian cancer [2 and 14]. The country with the highest incidence of ovarian cancer in 2020 was Brunei and the country with the highest rate of mortality due to ovarian cancer in 2020 was Samoa [14].

Ovarian cancer is often diagnosed at an advanced stage which leads to high rates of morbidity and mortality for patients. More than half of ovarian cancer cases are diagnosed at the metastatic stage which has a 5-year survival rate of 30.2%. To prevent this, effective strategies for early diagnosis need to be developed. Diagnosing ovarian cancer at an earlier stage would make it more curable. A high rate of recurrence occurs after the initial treatment of ovarian cancer, and these cases tend to be even less treatable. Due to this, new prevention and detection strategies along with treatment methods based

on the molecular characterization of ovarian cancer are needed [2]. Understanding how cell cycle dysregulation and perturbations in the DREAM complex affect ovarian cancer development and progression could provide insights into future detection and prevention strategies.

1.4 Study Hypothesis

In this study, we evaluated cell cycle gene expression in the ovarian cancer cell line, SKOV3, compared to immortalized pre-cancerous FT282 cells, and control human foreskin fibroblast BJ5Ta cells. We aim to better understand how cell cycle genes are regulated in cancer cells so that more effective molecular diagnostics for earlier detection of ovarian cancer can be designed. We hypothesize that cancer deregulates the expression of known DREAM target genes. With this in mind, we expected higher expression of cell cycle genes to be observed in SKOV3 and FT282 cells.

2 Materials

The cell lines SKOV3, FT282, and BJ5Ta were used for this experiment. The SKOV3 cell line has epithelial morphology and was isolated from a 64-year-old Caucasian woman [17]. FT282 is a cell line derived from fallopian tube secretory epithelial cells [20]. BJ5Ta is an immortalized foreskin fibroblast cell line isolated from a male patient [3].

Primers were used to target the early cell cycle genes hMYBL2, hMCM10, hMCM5, hCDC45, and hORC1. hMYBL2, also known as BMYB, encodes a protein that is a member of the MYB family of transcription factor genes [23]. hMCM10 encodes a protein involved in initiating eukaryotic genome replication [22]. The gene hMCM5 plays a role in DNA replication and is necessary for transcriptional activation [18]. The gene hCDC45 encodes a protein that is shown to interact with DNA polymerase alpha and the gene MCM7 [21]. hORC1 is essential for beginning DNA replication in eukaryotic cells [24].

Primers were used to target the housekeeping gene hU6. The small nuclear RNA hU6 forms some of the catalytic core of the spliceosome and interacts with other small nuclear RNAs and proteins during the splicing cycle [6]. This gene was chosen as the housekeeping gene since its expression is relatively constant throughout the cell cycle.

Primers were also used to target the late cell cycle genes hPRC1, hFOXM1, hTTK, hBUB1, and hCCNB2. hPRC1 encodes a protein involved in cytokinesis [25]. The gene hFOXM1 encodes a protein that is involved in cell proliferation as a transcriptional activator [8]. hTTK encodes a protein kinase that can phosphorylate tyrosine, serine, and

threonine. The protein encoded by this gene is associated with cell proliferation and an excess of this protein can lead to tumorigenesis [27]. The gene hBUB1 encodes a serine/threonine-protein kinase that plays a central role in mitosis and mutations in this gene are associated with various forms of cancer [26]. hCCNB2 is essential to the regulation of the cell cycle and may play a role in mediating cell cycle control through the transformation of growth factor beta [5].

Multiple medias and reagents were used throughout this experiment. Chloroform, isopropanol, ethanol, and nuclease-free water were used for the RNA isolation protocol. Nuclease-free water, a lithium chloride solution, and ethanol were used for the lithium chloride cleanup for the cell lines BJ5Ta and FT282. 10x RT buffer, 25x dNTP mix, 10x RT random primers, MultiScribe RTase, and nuclease-free water were used for RT protocol. 2x SYBR green, forward and reverse primers, and ddH2O were used to perform qPCR.

3 Methods

3.1 PAR Treatment

A combination of the CDK4/6 inhibitors palbociclib, abemaciclib, and ribociclib were used to treat the SKOV3, FT282, and BJ5Ta cell lines tested to achieve cell cycle arrest. These CDK4/6 inhibitors were then removed from all the plates used for these cells before three technical repeats were collected every two hours for ten hours following release from quiescence [19].

3.2 Primer Design

Primer sets were designed for the genes hFOXM1, hPRC1, hMYBL2, and hMCM10. First, the accession numbers were found for each gene using NCBI. Using primer BLAST, the PCR product was designed to be a minimum of 100bp and a maximum of 300bp. The primer pair is separated by a minimum of one intron on the corresponding genomic DNA. After the primers were generated, a primer pair near the 3' end of the gene was selected.

3.3 RNA Isolation

This was performed for all SKOV3, FT282, and BJ5Ta samples. The three technical repeats were collected at each time point during the time trial following the PAR treatment before being collected and stored in TRIZOL. TRIZOL reagent is used for total RNA isolation from the cells tested here. A Nanodrop was used to quantify the RNA content of all the samples tested.

3.4 LiCl RNA Cleanup

This step was performed for all BJ5Ta and FT282 samples used. Equal parts RNAse-free water and LiCl solution were added to each sample before being mixed and stored at -20C overnight. The next day, the samples were spun down, the liquid was removed, and ethanol/nuclease-free water was added back to the samples. The samples were spun down and the liquid was removed twice until they were completely dried. The samples were then rehydrated in nuclease-free water before the RNA levels were quantified using the Nanodrop.

3.5 RT

Based on the Nanodrop quantitation, which measured the amount of RNA in each sample tested, one microgram of RNA was combined with ddH2O, RT buffer, dNTP mix, RT random primers, and MultiScribe for cDNA RT. After running RT, the cDNA samples were diluted to a 1:10 ratio to be stored and tested with the primer pairs for the early and late stage genes for qPCR.

3.6 qPCR

For qPCR, forward and reverse primers for each gene were combined with SYBR Green and ddH2O before being run on a 96-well qPCR plate along with each sample. The primer pairs that were tested included those for the gene hU6 as a control, and the experimental genes hMYBL2, hMCM10, hMCM5, hCDC45, hORC1, hPRC1, hFOXM1, hTTK, hBUB1, and hCCNB2. For the BJ5Ta cell line, sample number 12 was lost before this step during RT and was not used for qPCR.

3.7 Statistical Analysis

The graphs showing relative quantity present the mean value at each time point of the gene in question in comparison to the control gene plus the standard error shown by the error bars. The graphs showing fold change present the mean in comparison to the value at time point P0 plus the standard error as shown by the error bars. A Student's T-test was run in comparison to the time point P0 for the graphs showing fold change. A value of $P<0.05$ was used to indicate a statistically significant result and is shown by *.

4 Results

To evaluate cell cycle gene regulation differences between cancer cells and normal cells, we tested the expression of early cell cycle genes (Figures 1-5) and late cell cycle genes (Figures 6-10). The early cell cycle genes tested include hMYBL2, hMCM10, hMCM5, hCDC45, and hORC1. The late cell cycle genes tested include hPRC1, hFOXM1, hTTK, hBUB1, and hCCNB2. In each figure, the results are presented for SKOV3, FT282, and BJ5Ta from left to right. We used hU6 as the control gene for all experimental measurement, since hU6 was expected to be expressed at the same level throughout the cell. We evaluated expression of cell cycle genes at the six time points indicating the number of hours after the cells were released from PAR treatment. These time points are labeled P0, P2, P4, P6, P8, and P10 to indicate zero, two, four, six, eight, and 10 hours after the removal of PAR.

We first compared early cell cycle gene expression between SKOV3 ovarian cancer cells and the FT282 and BJ5Ta control cell lines. We observed that the early cell cycle genes hMYBL2 and hMCM10 were both more highly expressed early in the cell cycle in the non-cancerous cell line with a lower relative quantity of these genes later in the cell cycle (Figures 1a and 2a). However, the fold change in quantity increased at a faster rate in both the cancerous and pre-cancerous cell lines tested (Figures 1b and 2b). The SKOV3 and FT282 cell lines do not follow the expression patterns that would be expected for the early cell cycle genes hMYBL2 and hMCM10. The early cell cycle genes hMCM5 and hCDC45 were both shown to increase in relative quantity as the cell cycle progressed in SKOV3 (Figures 3a and 4a). There was a positive trend in the fold

change in hMCM5 in SKOV3 before the fold change leveled off late in the cell cycle. However, the fold change was variable and showed no clear trend for the other two cell lines tested for hMCM5 (Figure 3b). The fold change was shown to be the greatest in the BJ5Ta cell line for the gene hCDC45 with the highest fold change late in the cell cycle. This same trend was seen in the two other cell lines tested as well (Figure 4b). The early cell cycle gene hORC1 was shown to have increased relative quantity from time point zero to six before gradually declining in the pre-cancerous and cancerous cell lines. However, the relative quantity observed in the SKOV3 cell line was greater than that in FT282 (Figure 5a). The fold change was shown to be the greatest in the BJ5Ta cell line with the highest levels late in the cell cycle (Figure 5b).

Next, we compared late cell cycle gene expression between SKOV3 ovarian cancer cells and the FT282 and BJ5Ta control cell lines. The gene hPRC1 was shown to have the greatest relative quantity late in the cell cycle in the cell line BJ5Ta while the gene hFOXM1 had the highest expression near the end of the early cell cycle (Figures 6a and 7a). The fold change was shown to increase later in the cell cycle for the cell lines SKOV3 and FT282 (Figures 6b and 7b). The fold change was higher in SKOV3 than FT282 for the gene hPRC1 and in FT282 for the gene hFOXM1 (Figures 6a and 7a). BJ5Ta does show what would be expected of late cell cycle gene expression for hPRC1, but not for hFOXM1. The late cell cycle gene hTTK is shown to have an overall positive trend in all three cell lines tested in relative quantity. There are greater relative quantities in the cancerous and pre-cancerous cell lines than the non-cancerous cell line tested (Figure 8a). The fold change of hTTK also shows an overall positive trend in the SKOV3

cell line (Figure 8b). There is a similar trend shown for the relative quantity of hBUB1 in the cell lines SKOV3 and FT282. However, the relative quantity of this gene was higher in the pre-cancerous cell line FT282 than in SKOV3 (Figure 9a). The fold change was relatively constant during the early part of the cell cycle and the peak fold change in all three cell lines occurred at some point late in the cell cycle (Figure 9b). The relative quantity of hCCNB2 followed similar trends to hBUB1, but there was a higher relative quantity of this gene in the cell line SKOV3 than in FT282 (Figure 10a). The fold change of hCCNB2 is similar to that of hBUB1 except for the peak in fold change in BJ5Ta (Figure 10b).

The non-cancerous cell line, BJ5Ta, followed the expected pattern with higher fold change near the beginning of the cell cycle for the early cell cycle genes hMYBL2 and hMCM10 (Figures 1b and 2b). The expected pattern would show a decrease in fold change later in the cell cycle. This pattern is not observed in any of the tested cell lines for the genes hMCM5, hCDC45, or hORC1 (Figures 3b, 4b, and 5b). Further attention should be paid to results with fold change values that were determined to be statistically significant in their difference from the values expected.

The cancerous and pre-cancerous cell lines SKOV3 and FT282 followed typical expression patterns of late cell cycle genes for the genes hPRC1 and hFOXM1 as shown by the increased fold change late in the cell cycle (Figures 6b and 7b). All three cell lines tested followed the expected expression patterns for the late cell cycle genes hTTK, hBUB1, and hCCNB2. The fold change for these genes peaked for all three cell lines late in the cell cycle as they were expected to (Figures 8b, 9b, and 10b).

4.1 Early Cell Cycle Genes

A)

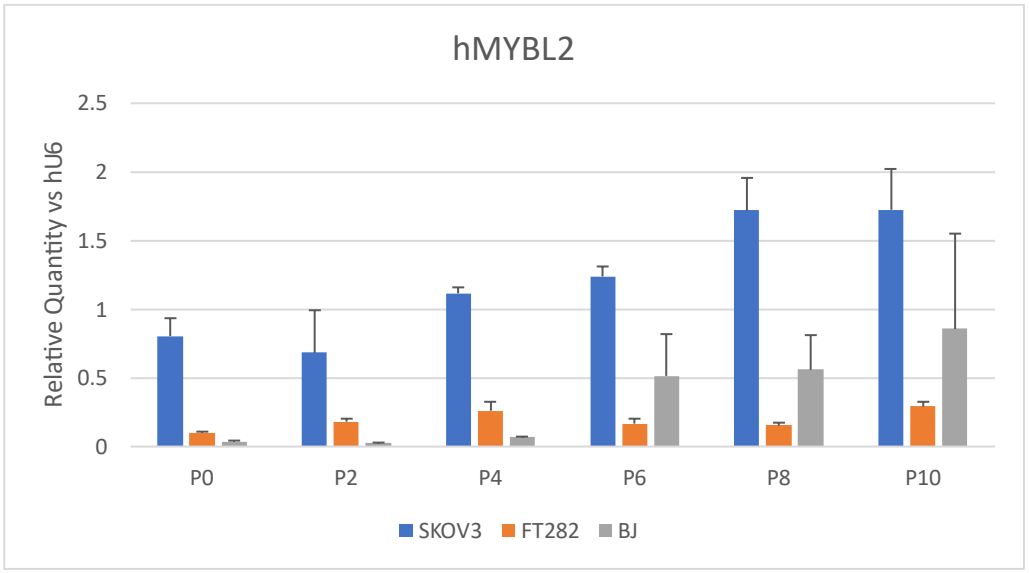

B)

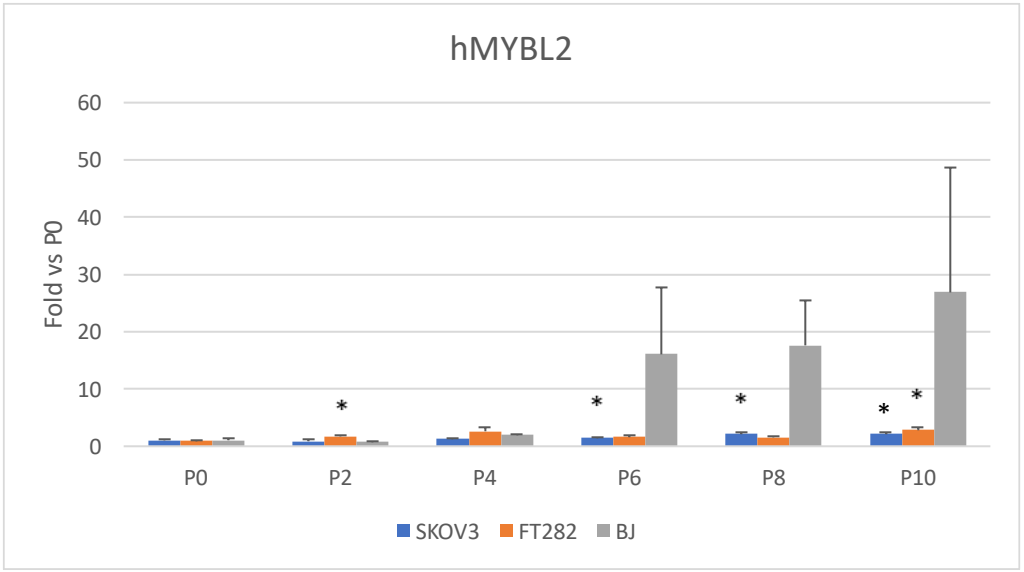

Figure 1: RT-qPCR results for the gene hMYBL2. A) Relative quantity of hMYBL2 is shown in comparison to gene hU6 at time points zero, two, four, six, eight, and 10 hours after release from quiescence. B) The fold change of hMYBL2 in comparison to time

zero is shown at time points zero, two, four, six, eight, and 10 hours after release from quiescence.

A)

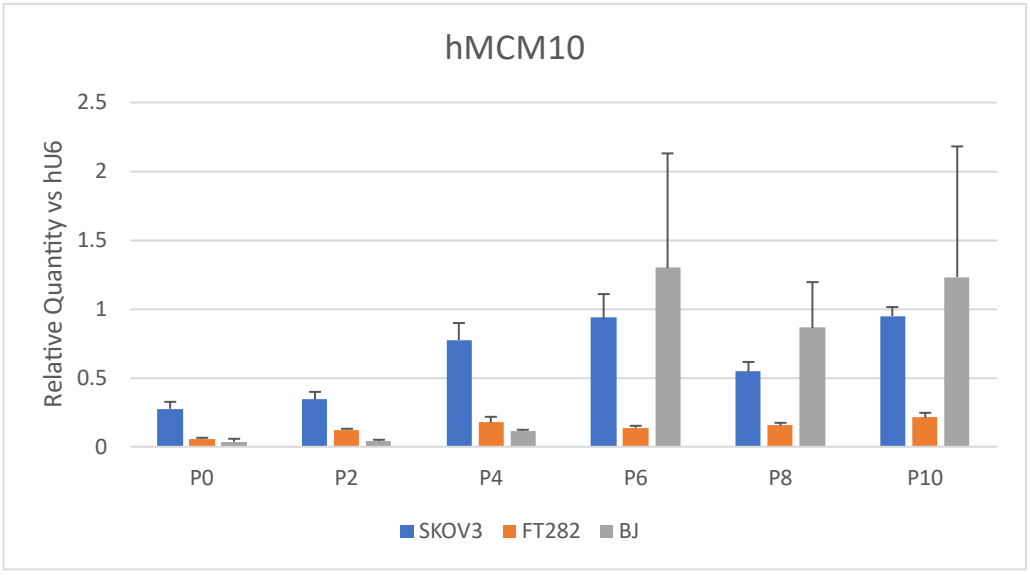

B)

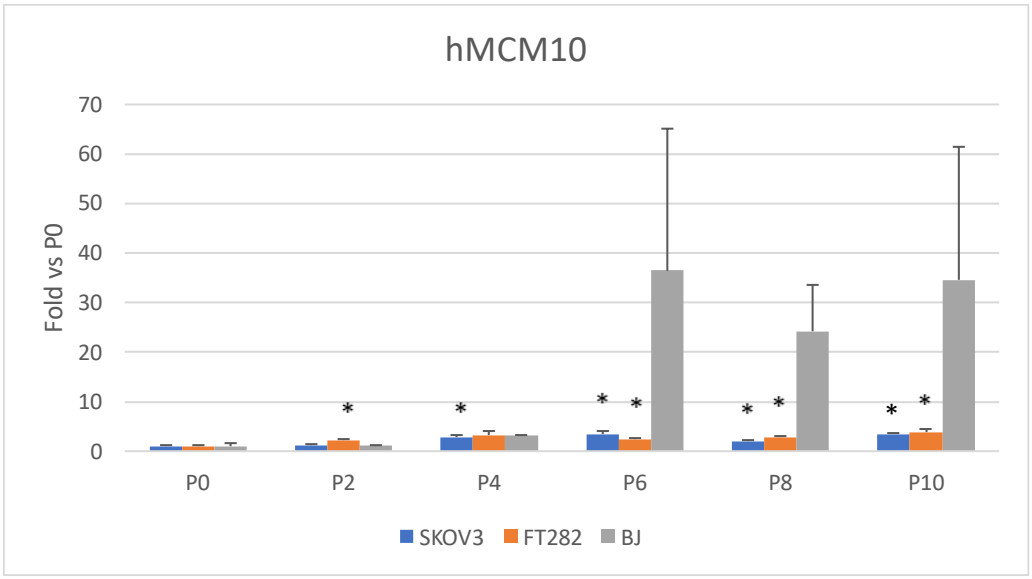

Figure 2: RT-qPCR results for the gene hMCM10. A) Relative quantity of hMCM10 is shown in comparison to gene hU6 at time points zero, two, four, six, eight, and 10 hours after release from quiescence. B) The fold change of hMCM10 in comparison to time zero is shown at time points zero, two, four, six, eight, and 10 hours after release from quiescence.

A)

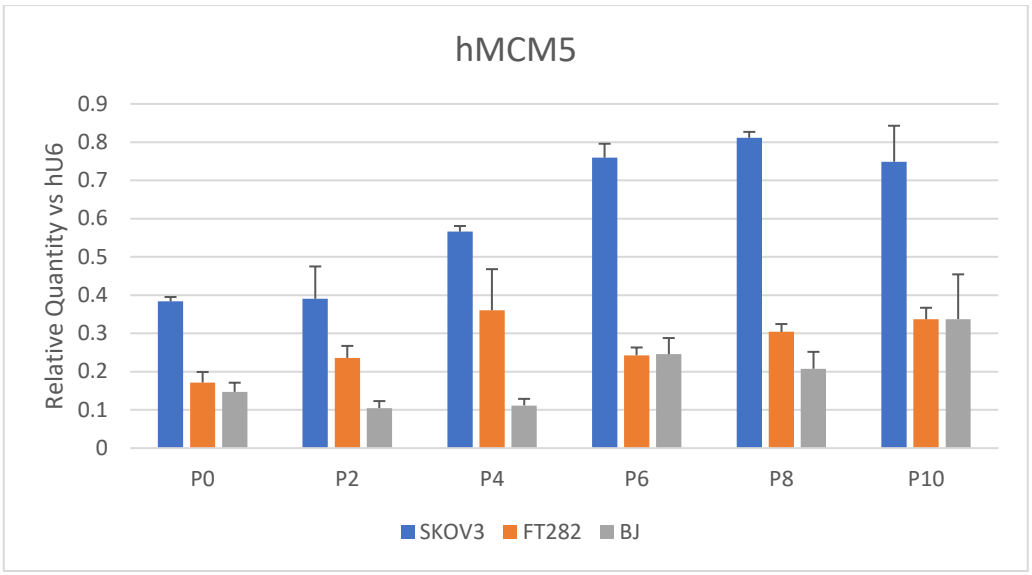

B)

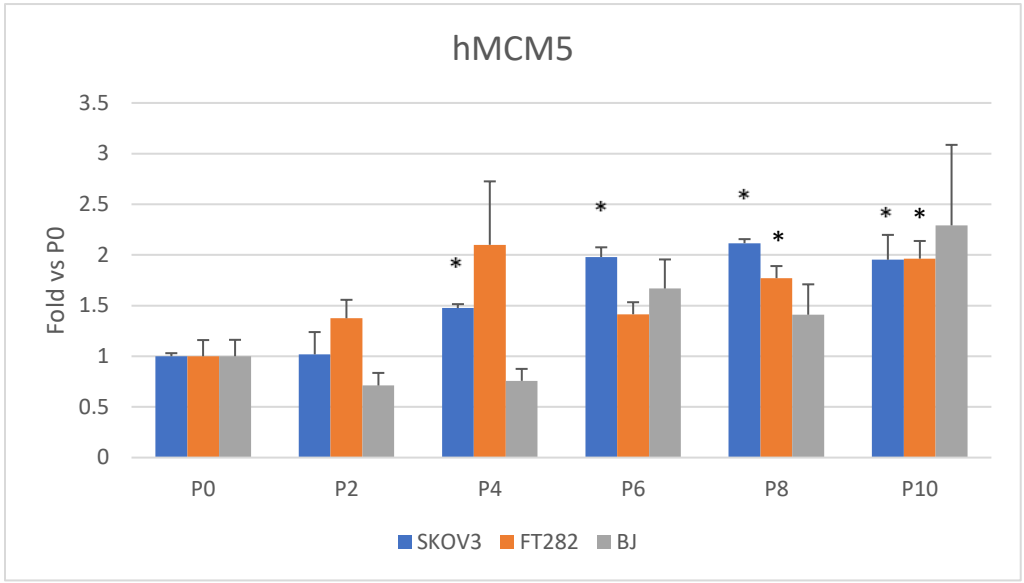

Figure 3: RT-qPCR results for the gene hMCM5. A) Relative quantity of hMCM5 is shown in comparison to gene hU6 at time points zero, two, four, six, eight, and 10 hours after release from quiescence. B) The fold change of hMCM5 in comparison to time zero is shown at time points zero, two, four, six, eight, and 10 hours after release from quiescence.

A)

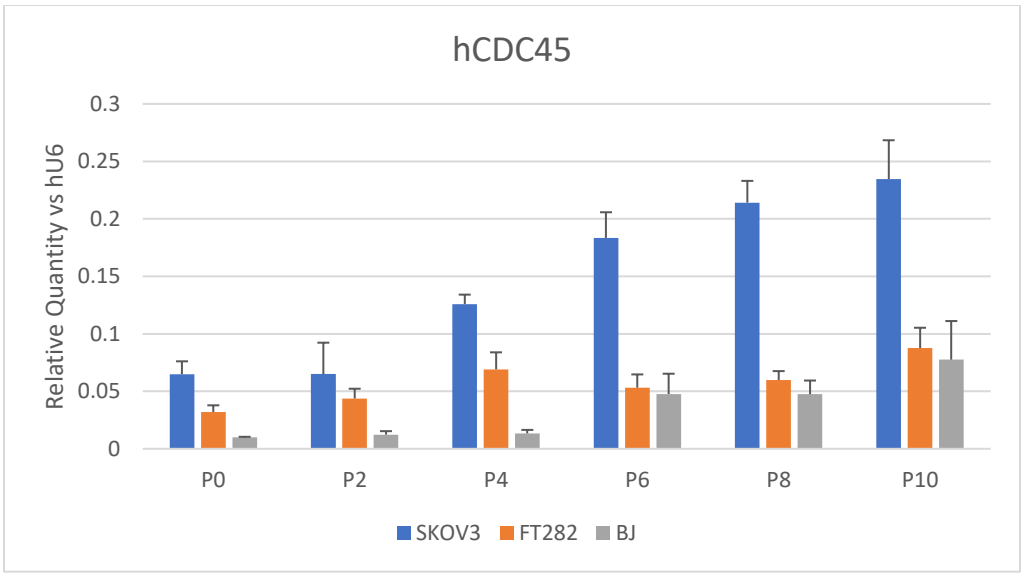

B)

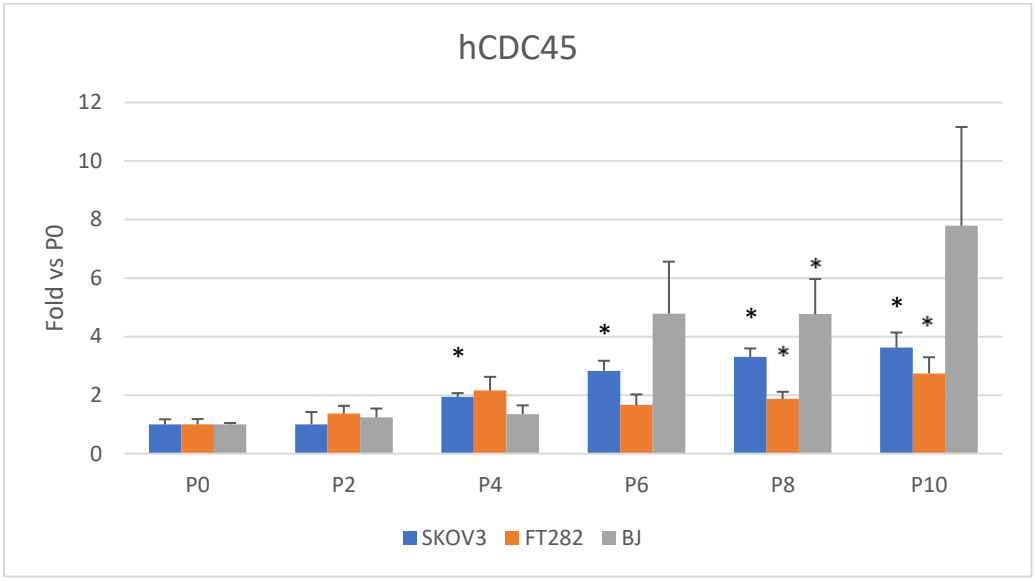

Figure 4: RT-qPCR results for the gene hCDC45. A) Relative quantity of hCDC45 is shown in comparison to gene hU6 at time points zero, two, four, six, eight, and 10 hours after release from quiescence. B) The fold change of hCDC45 in comparison to time zero

is shown at time points zero, two, four, six, eight, and 10 hours after release from quiescence.

A)

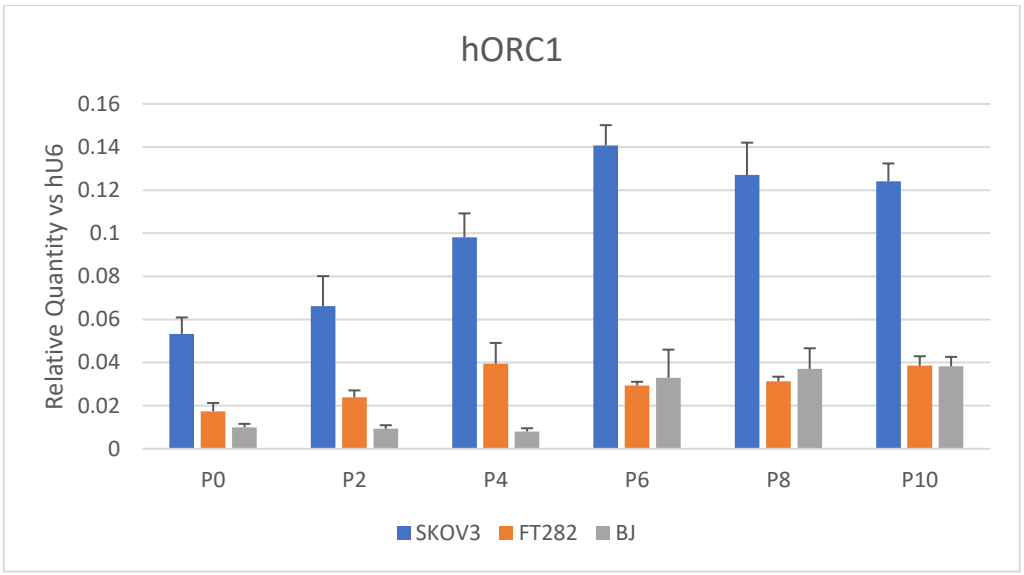

B)

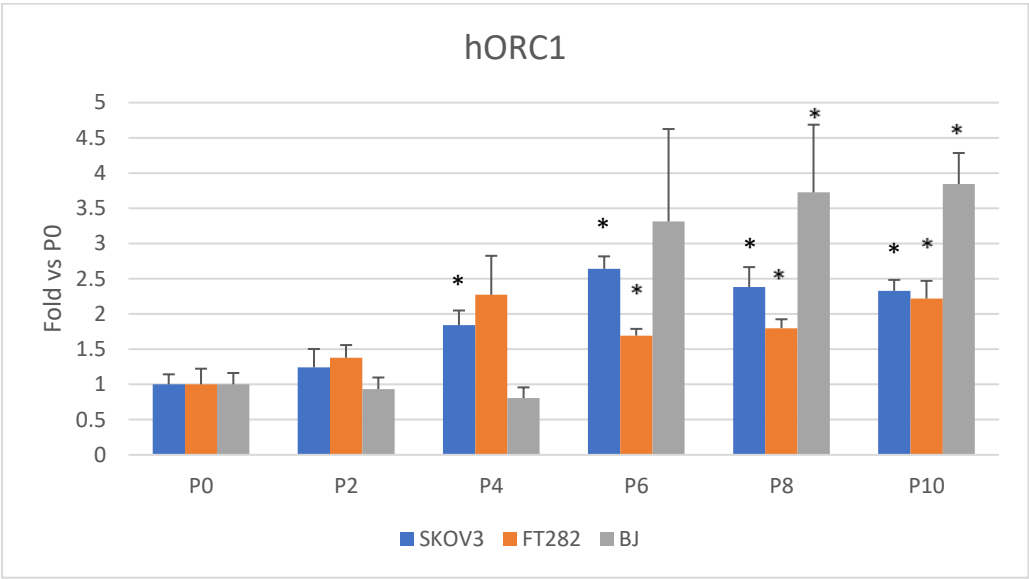

Figure 5: RT-qPCR results for the gene hORC1. A) Relative quantity of hORC1 is shown in comparison to gene hU6 at time points zero, two, four, six, eight, and 10 hours after release from quiescence. B) The fold change of hORC1 in comparison to time zero

is shown at time points zero, two, four, six, eight, and 10 hours after release from quiescence.

4.2 Late Cell Cycle Genes

A)

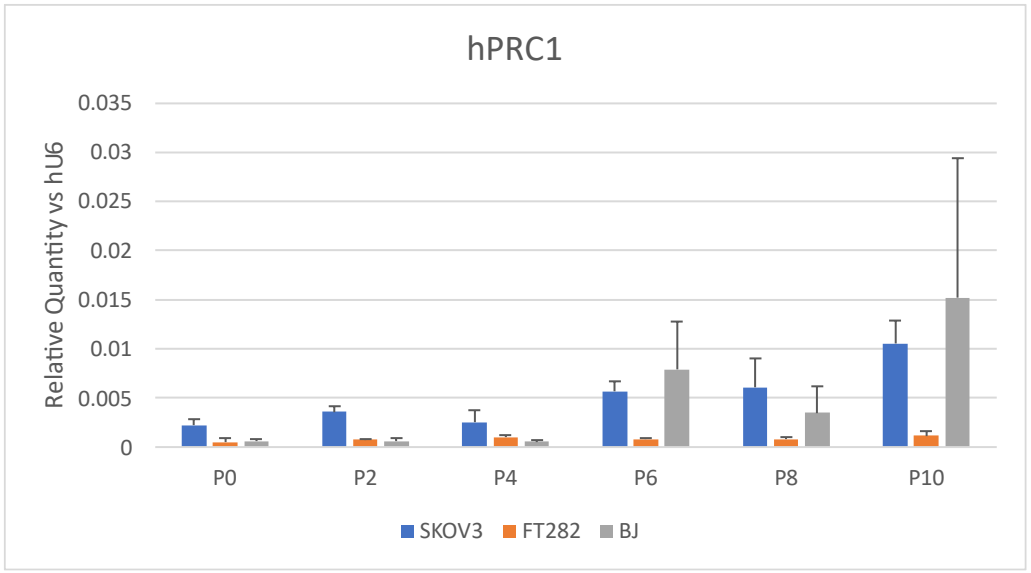

B)

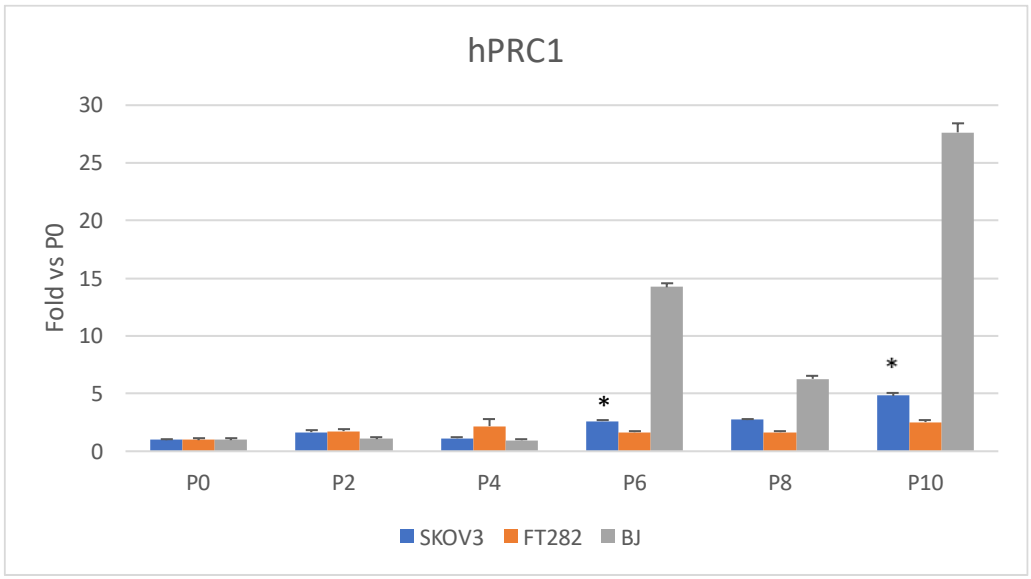

Figure 6: RT-qPCR results for the gene hPRC1. A) Relative quantity of hPRC1 is shown in comparison to gene hU6 at time points zero, two, four, six, eight, and 10 hours after release from quiescence. B) The fold change of hPRC1 in comparison to time zero is

shown at time points zero, two, four, six, eight, and 10 hours after release from quiescence.

A)

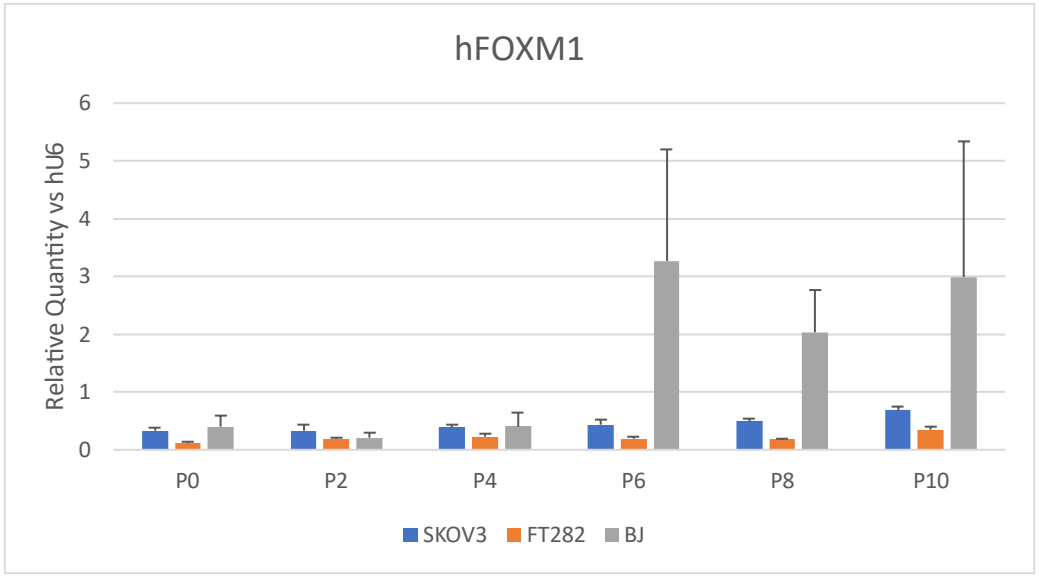

B)

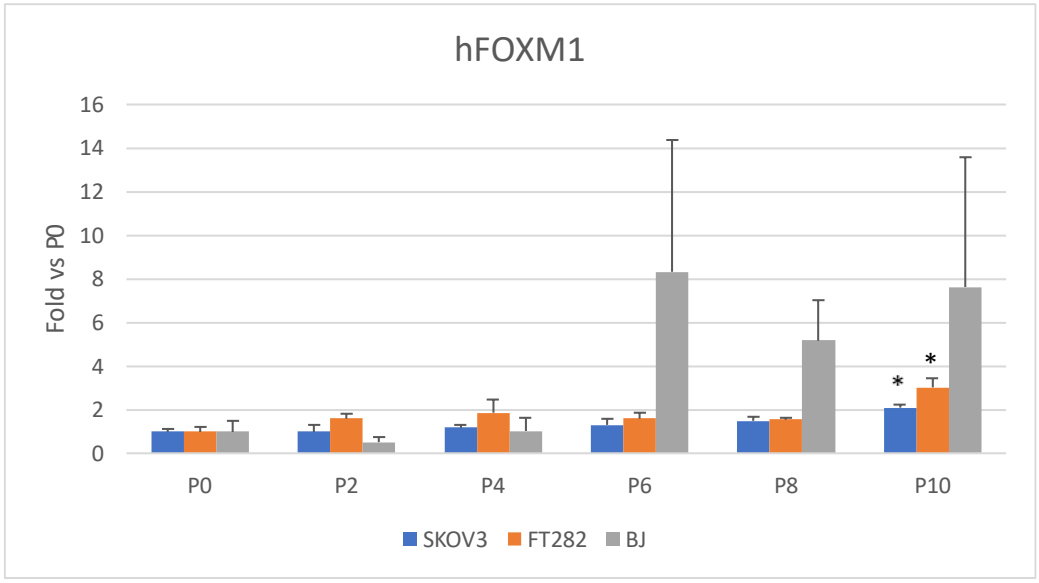

Figure 7: RT-qPCR results for the gene hFOXM1. A) Relative quantity of hFOXM1 is shown in comparison to gene hU6 at time points zero, two, four, six, eight, and 10 hours after release from quiescence. B) The fold change of hFOXM1 in comparison

to time zero is shown at time points zero, two, four, six, eight, and 10 hours after release from quiescence.

A)

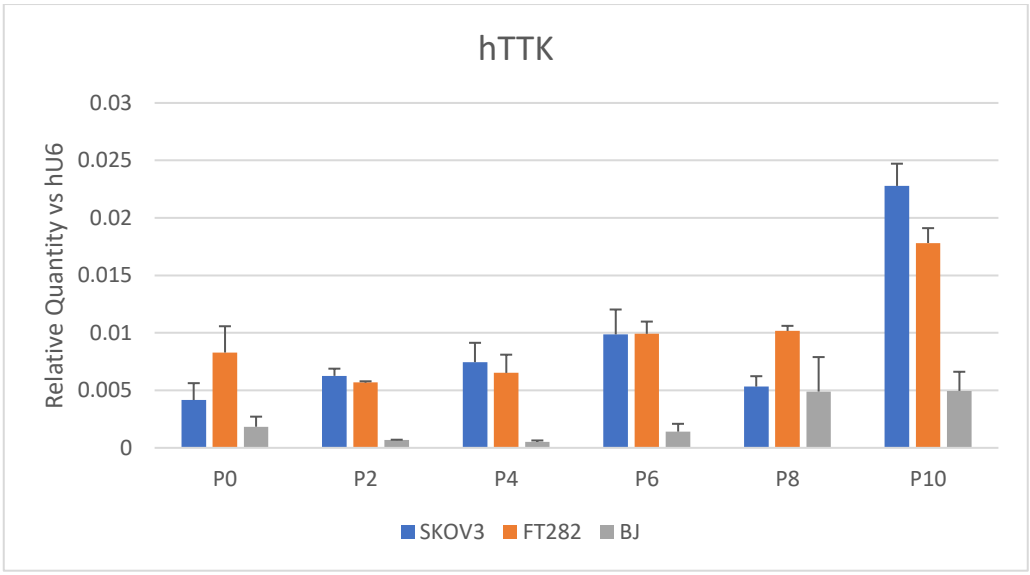

B)

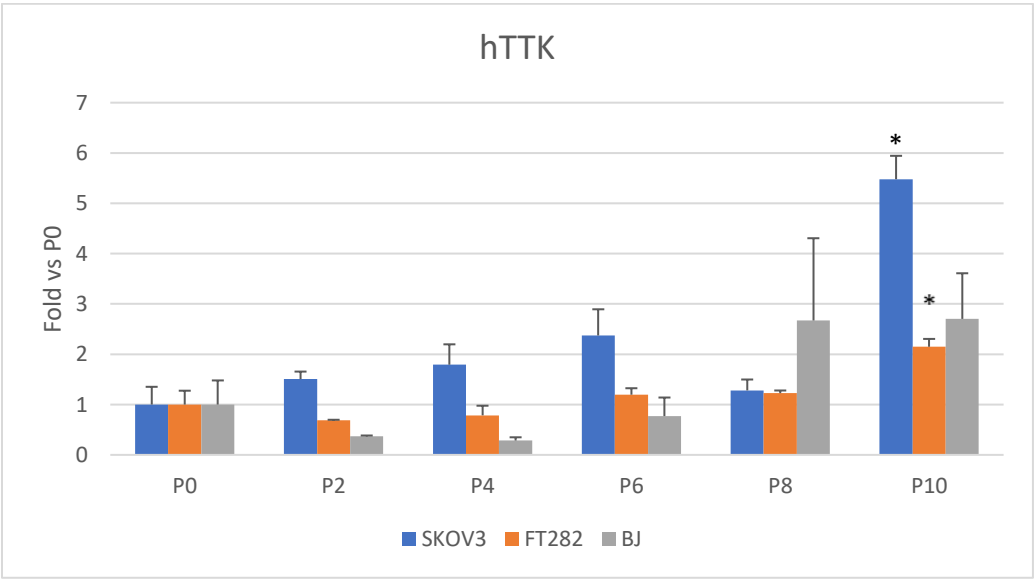

Figure 8: RT-qPCR results for the gene hTTK. A) Relative quantity of hTTK is shown in comparison to gene hU6 at time points zero, two, four, six, eight, and 10 hours after release from quiescence. B) The fold change of hTTK in comparison to time zero is

shown at time points zero, two, four, six, eight, and 10 hours after release from quiescence.

A)

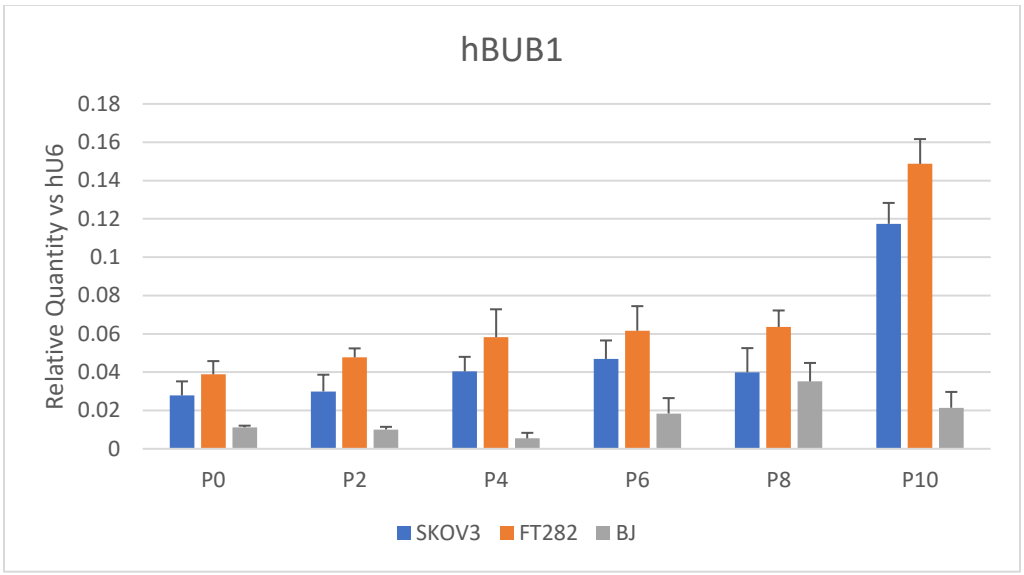

B)

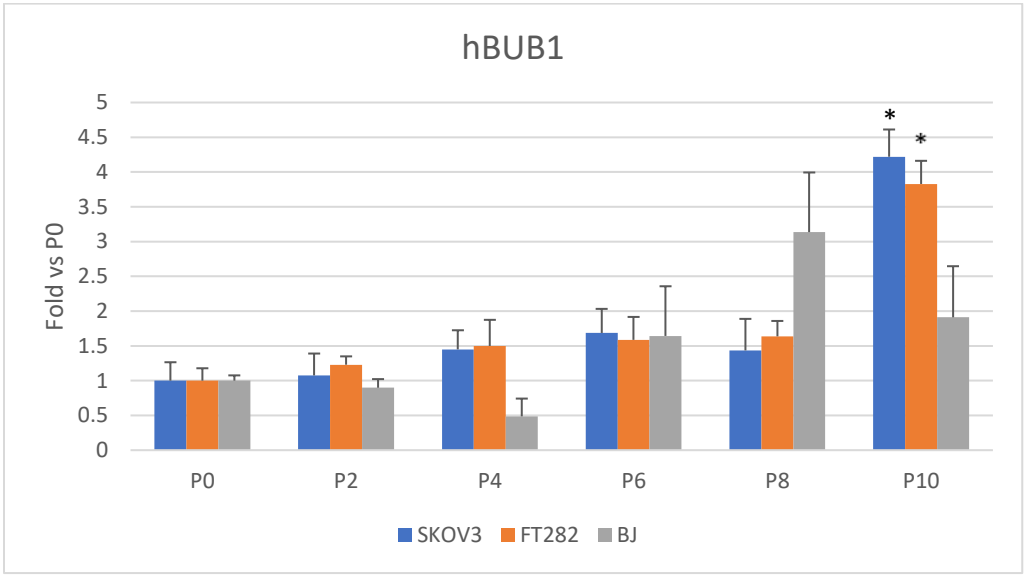

Figure 9: RT-qPCR results for the gene hBUB1. A) Relative quantity of hBUB1 is shown in comparison to gene hU6 at time points zero, two, four, six, eight, and 10 hours after release from quiescence. B) The fold change of hBUB1 in comparison to time zero is shown at time points zero, two, four, six, eight, and 10 hours after release from quiescence.

A)

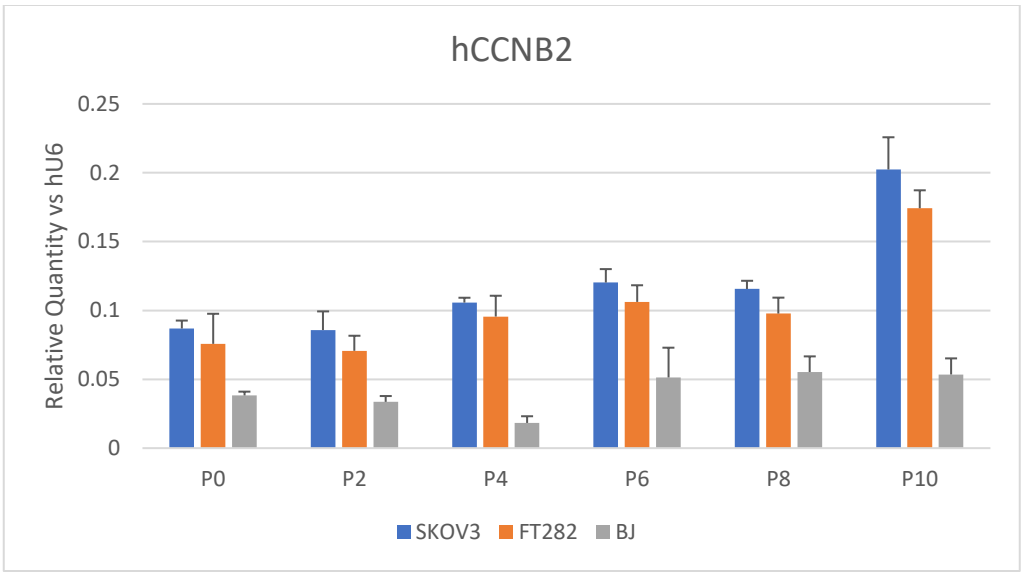

B)

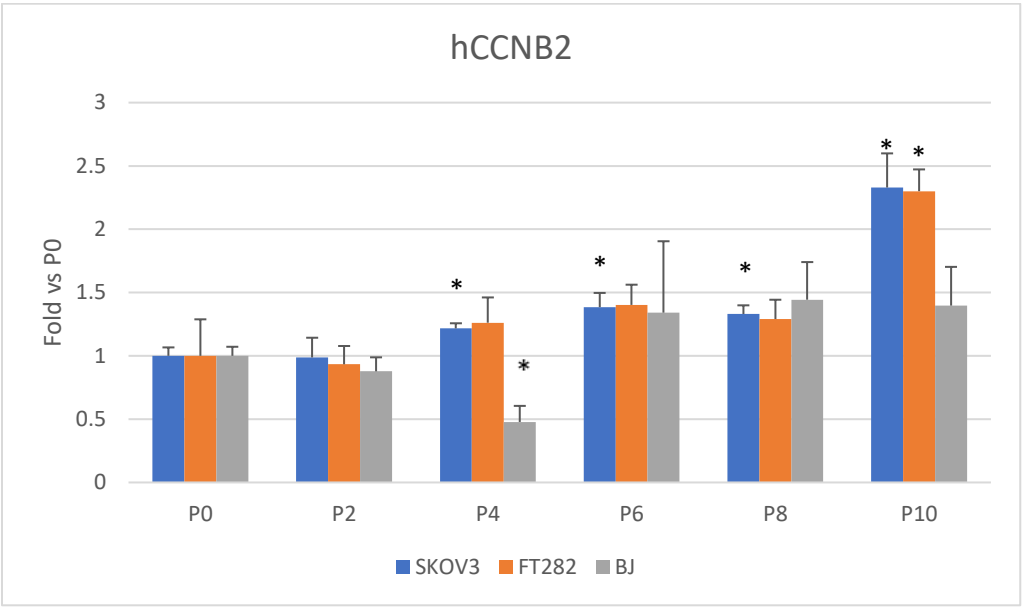

Figure 10: RT-qPCR results for the gene hCCNB2. A) The relative quantity of hCCNB2 is shown in comparison to gene hU6 at time points zero, two, four, six, eight, and 10 hours after release from quiescence. B) The fold change of hCCNB2 in comparison to

time zero is shown at time points zero, two, four, six, eight, and 10 hours after release from quiescence.

5 Discussion

Many of the early cell cycle genes that were tested in this experiment behaved differently than what was expected. For the gene hMYBL2, even though this is an early cell cycle gene, peak fold change in the cell line SKOV3 happened late in the cell cycle. The gene hMCM10 had a peak in fold change in the expected range as well as a similar peak late in the cell cycle for the cell lines SKOV3 and FT282. For the early cell cycle genes hMCM5 and hCDC45, the fold change increased before leveling off late in the cell cycle for the cell line SKOV3. These patterns are all outside of what would be expected for early cell cycle gene expression. Peak fold increase in these early cell cycle genes occurring late in the cell cycle is unusual since these genes are expected to have peak expression early in the cell cycle. Therefore, it would be expected that the fold change would decrease for these genes late in the cell cycle.

Particular attention should be paid to the pre-cancerous cell line FT282 to see if this cell line behaves more similarly to the cancerous cell line SKOV3, or the non-cancerous cell line BJ5Ta. The trends seen in the figures for relative quantity of FT282 in comparison to SKOV3 and BJ5Ta does not always follow the same trend in the corresponding figure displaying fold change for the same gene. RNA sequencing results for these early and late cell cycle genes would provide more information on whether FT282 has more similar gene expression patterns to SKOV3 or BJ5Ta for these genes.

Further attention should be paid to results with fold change values that were determined to be statistically significant in their difference from the values expected.

These differences that were observed in the fold change values suggest that the cell cycle is not being properly regulated under these conditions. The dysregulation in the expression of these cell cycle genes could be due to perturbations in the DREAM complex and its role in repressing cell cycle genes, or due to perturbations in Rb. The DREAM complex plays a repressive role in the cell cycle which makes it important for quiescence, so perturbations in DREAM could cause proliferation to be favored. This shift toward proliferation could be due to the balance between the DREAM complex and BMYB-MuvB-FOXM1 being disturbed in cancer cells [16].

The regulation of early cell cycle gene expression involves repression through the binding of Rb to activator E2Fs and DREAM E2Fs binding to DNA E2F recognition elements. This regulation can be disrupted if Rb is phosphorylated which reduces the repression of activator E2Fs and expression of early cell cycle genes. In addition to this phosphorylation, DREAM repression is disrupted through the phosphorylation of p130. The regulation of late cell cycle gene expression is coordinated by the CDK phosphorylation of BMYB and FOXM1. BMYB may play a limited role in activating MuvB target genes, and instead primarily works with MuvB to recruit FOXM1 to G2/M promoters [7].

There were some limitations that we faced when conducting these experiments including the cell lines having different properties and undergoing different treatments. The cancerous and pre-cancerous cell lines are epithelial based while the non-cancerous cell line is composed of fibroblast cells. Epithelial and fibroblast cells have different

properties which could have contributed to some of the differences observed here in cell cycle gene expression. For example, epithelial cells are tightly connected to one another and arranged in a monolayer while fibroblast cells form the supportive framework for these epithelial cells. In addition to this, fibroblast cells can migrate as individual cells which epithelial cells are unable to do [10]. These cell lines were treated in the same ways aside from the LiCl cleanup that was performed on the pre-cancerous and non-cancerous cell lines. This lithium chloride cleanup was performed for the FT282 and BJ5Ta cell lines to help clean up the samples before downstream processing in qPCR, but also resulted in a loss of RNA. This loss in RNA could have led to some issues when running qPCR. This difference in treatment could have also led to some differences when comparing results between the three cell lines.

6 Conclusion

For further analysis, RNA sequencing will be performed for the cell cycle genes used in this experiment for the cell lines tested here to quantify gene expression levels. RNA sequencing has been shown to have high levels of accuracy in quantifying gene expression levels. Therefore, this technology could be used to quantify the expression levels of the early and late cell cycle genes that were tested for this experiment [28]. This additional information would allow for more accurate interpretation of how the expression of these cell cycle genes differs between cancerous, pre-cancerous, and non-cancerous cell lines. In addition to this, the time release could be extended beyond the ten-hour point to expand the view of the late stages of the cell cycle. Only one time point beyond what is shown in this experiment would need to be included to give this more complete view of the late stages of the cell cycle. This would provide further insight if the cell lines were not all synchronized upon their release from quiescence. This could have occurred if the culture conditions were not sufficient for synchronization to occur during the PAR treatment [19].

In many of the cell cycle genes tested with SKOV3, proliferation was favored as shown by the relative quantities compared to the control gene. The balance between the DREAM and BMYB-MuvB-FOXM1 complexes is often disturbed in cells that have become cancerous and favor cell proliferation [16]. It is not known if this shift in balance between these two complexes occurs in ovarian cancer cells. Determining if DREAM perturbations are responsible for the shift towards proliferation observed in SKOV3 could provide insight into future prevention and detection strategies for ovarian cancer.

FT282 had similar fold change patterns to SKOV3 for some of the cell cycle genes tested, but not all of them. Many of the cell cycle genes tested were upregulated, but the reason for this upregulation is not known. Determining if this shift toward proliferation is due to a disturbance in the balance between DREAM and BMYB-MuvB-FOXM1 could provide more information about whether FT282 behaves more similarly to SKOV3 or BJ5Ta.

7 Reference List

[1] Alberts B, Johnson A, Lewis J, et al. Molecular Biology of the Cell. 4th edition. New York: Garland Science; 2002. An Overview of the Cell Cycle. Available from: https://www.ncbi.nlm.nih.gov/books/NBK26869/

[2] Arora T, Mullangi S, Lekkala MR. Ovarian Cancer. [Updated 2023 Jan 2]. In: StatPearls [Internet]. Treasure Island (FL): StatPearls Publishing; 2023 Jan-. Available from: https://www.ncbi.nlm.nih.gov/books/NBK567760/

[3] BJ-5ta - CRL-4001 | ATCC. (n.d.). https://www.atcc.org/products/crl-4001

[4] *Cancer of the ovary - cancer stat facts*. SEER. (n.d.). https://seer.cancer.gov/statfacts/html/ovary.html

[5] *CCNB2 gene - genecards | CCNB2 protein | CCNB2 antibody*. Gene Cards. (2023, May 21). https://www.genecards.org/cgi-bin/carddisp.pl?gene=CCNB2

[6] Didychuk1, A. L., & and, S. E. B. (1970, January 1). *Allison L. Didychuk*. RNA. https://rnajournal.cshlp.org/content/24/4/437.abstract

[7] Fischer, M., Schade, A. E., Branigan, T. B., Muller, G. A., & DeCaprio, J. A. (2022, July 11). *Coordinating gene expression during the cell cycle*. Trends in Biochemical Sciences. https://www.cell.com/trends/biochemical-sciences/fulltext/S0968-0004(22)00148-7

[8] *FOXM1 gene - genecards | FOXM1 protein | foxm1 antibody*. Gene Cards. (2023, May 22). https://www.genecards.org/cgi-bin/carddisp.pl?gene=FOXM1

[9] Mages, C. F., Wintsche, A., Bernhart, S. H., & Müller, G. A. (2017). The DREAM complex through its subunit Lin37 cooperates with Rb to initiate quiescence. *eLife*, *6*, e26876. https://doi.org/10.7554/eLife.26876

[10] Mallinjoud, P., Villemin, J. P., Mortada, H., Polay Espinoza, M., Desmet, F. O., Samaan, S., Chautard, E., Tranchevent, L. C., & Auboeuf, D. (2014). Endothelial, epithelial, and fibroblast cells exhibit specific splicing programs independently of their tissue of origin. *Genome research*, *24*(3), 511–521. https://doi.org/10.1101/gr.162933.113

[11] Marescal, O., & Cheeseman, I. M. (2020). Cellular Mechanisms and Regulation of Quiescence. *Developmental cell*, *55*(3), 259–271. https://doi.org/10.1016/j.devcel.2020.09.029

[12] Mercadante AA, Kasi A. Genetics, Cancer Cell Cycle Phases. [Updated 2022 Aug 8]. In: StatPearls [Internet]. Treasure Island (FL): StatPearls Publishing; 2023 Jan-. Available from: https://www.ncbi.nlm.nih.gov/books/NBK563158/

[13] *Ovarian cancer incidence statistics*. Cancer Research UK. (2022, March 11). https://www.cancerresearchuk.org/health-professional/cancer-statistics/statistics-by-cancer-type/ovarian-cancer/incidence#heading-One

[14] *Ovarian cancer statistics: World cancer research fund international*. WCRF International. (2022, April 14). https://www.wcrf.org/cancer-trends/ovarian-cancer-statistics/

[15] Phung, M. T., Pearce, C. L., Meza, R., & Jeon, J. (2023). Trends of Ovarian Cancer Incidence by Histotype and Race/Ethnicity in the United States 1992-2019. *Cancer research communications*, *3*(1), 1–8. https://doi.org/10.1158/2767-9764.CRC-22-0410

[16] Sadasivam, S., & DeCaprio, J. A. (2013). The DREAM complex: master coordinator of cell cycle-dependent gene expression. *Nature reviews. Cancer*, *13*(8), 585–595. https://doi.org/10.1038/nrc3556

[17] *SK-OV-3 [Skov-3; SKOV3] - HTB-77 | ATCC*. American Type Culture Collection. (n.d.). https://www.atcc.org/products/htb-77

[18] Snyder, M., He, W., & Zhang, J. (2005, September 30). *The DNA replication factor MCM5 is essential for Stat1-mediated transcriptional activation*. PNAS. https://www.pnas.org/doi/10.1073/pnas.0507479102

[19] Trotter, E. W., & Hagan, I. M. (2020, October). *Release from cell cycle arrest with CDK4/6 inhibitors generates highly ...* Open Biology. https://royalsocietypublishing.org/doi/10.1098/rsob.200200

[20] U.S. National Library of Medicine. (2022, February 15). *Geo accession viewer*. National Center for Biotechnology Information. https://www.ncbi.nlm.nih.gov/geo/query/acc.cgi?acc=GSM5225865

[21] U.S. National Library of Medicine. (2023, June 21). *CDC45 cell division cycle 45 [Homo Sapiens (human)] - gene - NCBI*. National Center for Biotechnology Information. https://www.ncbi.nlm.nih.gov/gene/8318

[22] U.S. National Library of Medicine. (2023, June 21). *MCM10 minichromosome maintenance 10 replication initiation factor [homo sapiens (human)] - gene - NCBI*. National Center for Biotechnology Information. https://www.ncbi.nlm.nih.gov/gene/55388

[23] U.S. National Library of Medicine. (2023, June 21). *MYBL2 MYB proto-oncogene like 2 [homo sapiens (human)] - gene - NCBI*. National Center for Biotechnology Information. https://www.ncbi.nlm.nih.gov/gene/4605

[24] U.S. National Library of Medicine. (2023, June 21). *Orc1 origin recognition complex subunit 1 [homo sapiens (human)] - gene - NCBI*. National Center for Biotechnology Information. https://www.ncbi.nlm.nih.gov/gene/4998

[25] U.S. National Library of Medicine. (2023, June 21). *PRC1 protein regulator of cytokinesis 1 [homo sapiens (human)] - gene - NCBI*. National Center for Biotechnology Information. https://www.ncbi.nlm.nih.gov/gene/9055#:~:text=PRC1%20is%20a%20microtubule%2Dassociated,by%20p53%20via%20regulating%20cytokinesis

[26] U.S. National Library of Medicine. (n.d.-b). *Bub1 bub1 mitotic checkpoint serine/threonine kinase [Homo Sapiens (human)] - gene - NCBI*. National Center for Biotechnology Information. https://www.ncbi.nlm.nih.gov/gene/699

[27] U.S. National Library of Medicine. (n.d.-c). *TTK ttk protein kinase [homo sapiens (human)] - gene - NCBI*. National Center for Biotechnology Information. https://www.ncbi.nlm.nih.gov/gene/7272

[28] Wang, Z., Gerstein, M., & Snyder, M. (2009, January). *RNA-seq: A revolutionary tool for transcriptomics*. Nature reviews. Genetics. https://www.ncbi.nlm.nih.gov/pmc/articles/PMC2949280/

[29] Whitfield, M. L., Sherlock, G., Saldanha, A. J., Murray, J. I., Ball, C. A., Alexander, K. E., Matese, J. C., Perou, C. M., Hurt, M. M., Brown, P. O., & Botstein, D. (2002). Identification of genes periodically expressed in the human cell cycle and their expression in tumors. *Molecular biology of the cell, 13*(6), 1977–2000. https://doi.org/10.1091/mbc.02-02-0030